Dexterous Grippers: Putting Nonholonomy to Work for Fine Manipulation

Antonio Bicchi, Alessia Marigo

Keywords— **Robotic hands, Dexterous manipulation, Shape reconstruction, Motion Planning, Nonholonomic systems.**

Abstract— **In this paper, we describe the realization and control of robotic end–effectors that are designed to achieve high operational versatility with limited constructive complexity. The design of such end–effectors, which can be regarded either as low–complexity robot hands or as highly versatile robot grippers, is based on the intentional exploitation of nonholonomic effects that occur in rolling. While the potential usefulness of manipulation by rolling has been theoretically established in the literature, several problems in the practical implementation of the concept remained open. In particular, manipulation of parts of complex, and *a priori* unknown shape, is considered in this paper. Experimental low-complexity grippers that realize dexterous manipulation by rolling are also described.**

I. Introduction

The development of mechanical hands for grasping and fine manipulation of objects has been an important part of robotics research since its beginnings. Comparison of the amazing dexterity of the human hand with the extremely elementary functions performed by industrial grippers, compelled many robotics researchers to try and bring some of the versatility of the anthropomorphic model in robotic devices. From the relatively large effort spent by the research community towards this goal, several robot hands sprung out in laboratories all over the world ([1] contains a recent survey).

Multifingered, "dextrous" robot hands often featured very advanced mechanical design, sensing and actuating systems, and also proposed interesting analysis and control problems, concerning e.g. the distribution of control action among several fingers subject to complex nonlinear bounds such as those due to friction. Notwithstanding the fact that hands designed in that phase of research were often superb engineering projects, the community had to face a very poor penetration to the factory floor, or to any other scale application. Among the various reasons for this, there is undoubtedly the fact that dextrous robot hands were too mechanically complex to be industrially viable in terms of cost, weight, and reliability.

Reacting to this observation, several researchers started to reconsider the problem of obtaining good grasping and manipulation performance by using mechanically simpler devices. This approach can be seen as an embodiment of a more general, "minimalist" attitude at robotics design (see e.g. works reported in [2]). It often turns out that this is indeed possible, provided that more sophisticated analysis, programming and control tools are employed. The challenge is to make available theoretical tools which allow to reduce the hardware cost at a - comparatively little - incremental cost of basic research.

In this paper, we will focus on the achievement of dexterity with simplified hardware. By dexterity we mean here (in a somewhat restrictive sense) the ability of a hand to relocate and reorient an object being manipulated among its fingers, without loosing the grasp on it. Salisbury ([3]) observed that a hand that manipulates an object by means of rigid, hard–finger, non–rolling and non–sliding contacts, needs at least three fingers, and three joints per finger, to achieve dexterity. As a consequence, most dexterous robotic hands use at least nine independent joints, which fact entails complex, costly and hard-to-maintain apparatuses for actuation and sensing.

If the non–rolling assumption is lifted, however, the situation changes dramatically, as nonholonomy enters the picture. The analysis of manipulation in the presence of rolling has been pioniereed by Montana [4] and Cai and Roth [5]. Subsequently, Cole, Hauser, and Sastry [6] considered the kinematics and control of a multifingered hand with rolling contacts. Li and Canny [7] used nonlinear controllability tools to show that a sphere rolling on a plane, or on another sphere, can be relocated and reoriented at will by using only rolling motions. A first prototype of a hand implementing purposefully rolling manipulation was presented in [8] (see fig.8), along with a numeric algorithm for planning. Controllability of rolling for smooth, strictly convex, axial–symmetric surfaces rolling on planes was shown in [9]. A general result was presented in [10], showing the generic controllability of rolling pairs (i.e., that any two surfaces, with the only exception of surfaces that are mirror images of each other, can be arbitrarily reoriented and relocated by rolling). While the above results were limited to rolling surfaces with smooth surface, the case where the object to be manipulated had a polyhedral description was considered in ([11],[12]).

Such theoretical results proved in principle the feasibility of exploiting rolling manipulation to enhance dexterity and to reduce the complexity, cost, weight, and unreliability of the hardware used in robotic hands. However, in order for such promises of the nonholonomy-on-purpose approach to be fulfilled in practice, much work remains to be done. In particular, there is a need for efficient and robust algorithms and techniques to deal with manipulation of ob-

Manuscript submitted May, 2001. This work was conducted with partial support of MURST grant "Mistral".

Antonio Bicchi is with the Interdept. Research Center "Enrico Piaggio", University of Pisa, via Diotisalvi, 2, 56100 Pisa, Italy. Phone: +39050553639. Fax:+39050550650. Alessia Marigo is with the Int. School for Advanced Studies (SISSA-ISAS), Trieste, Italy. E–mail: bicchi@ing.unipi.it, marigo@piaggio.ccii.unipi.it

jects that realistically can be encountered in applications, and for practical devices adding to the normal functions of a robot gripper new manipulative features.

In this paper we attack some of the most important open problems in the manipulation by rolling of objects, from both a theoretical and practical point of view. After some background review (II), in section III, we consider manipulating objects for a which a geometric description is not available a priori, and provide an algorithm for reconstructing their shape based on sensing information collected during manipulation, taking into account the smoothness requirements deriving from subsequent application of reconstructed models to planning. In section IV, we consider planning rolling manipulation of objects of general shape. A novel algorithm is proposed that improves upon existing techniques in that: i) it is finitely computable and predictable (an upper bound on the computations necessary to reach a given goal within a tolerance can be given), and ii) it possesses a topological property which enables obstacles and workspace limitations to be dealt with in an effective way. In V), we present the design of a novel dexterous gripper (DxGrip–II) that is intended to be a practical substitution of existing end–effectors at least in light–weight robotic applications. Experimental results are reported that confirm the validity of proposed technique in practical applications.

II. Background

For the reader's convenience, we report here some preliminaries that help in fixing the notation and resume the background. For more details, see e.g. [13]. We will consider both the part to be manipulated (henceforth referred to as "object") and the manipulating "finger" to be simple regular surfaces, denoted as Σ_o and Σ_f, respectively. Let the two surfaces be described, in a neighborhood of the contact point, by orthogonal parameterizations (f_i, U_i); $f_i : U_i \subset \mathbb{R}^2 \to \Sigma_i \subset \mathbb{R}^3$, $(i = f, o)$, and let $u = (u_1, u_2) \in U_o$, $x = (x_1, x_2) \in U_f$ denote the local coordinates. A Gauss (normal) map $n_i : \Sigma_i \to S^2 \subset \mathbb{R}^3$, can be written for both surfaces as $n_i = \frac{f_{i,1} \times f_{i,2}}{\|f_{i,1} \times f_{i,2}\|}$). It is useful to define a normalized Gauss frame with unit vectors $\{(f_{i,1}/\|f_{i,1}\|), (f_{i,2}/\|f_{i,2}\|), (n_i)\}$.

The kinematic equations of motion for rolling bodies describe the evolution of the (local) coordinates of the contact point on the surfaces, u and x, along with the (holonomy) angle ψ between the two Gauss frames, as they change according to the rigid relative motion of the finger and the object described by the relative velocity v and angular velocity $\omega = (\omega_x, \omega_y, \omega_z)$.

Accordingly, the (local) state for our problem is comprised of the coordinates of the contact point on the object ($u \in \mathbb{R}^2$) and on the finger ($x \in \mathbb{R}^2$), along with the holonomy angle $\psi \in S^1$. A distance on the resulting state manifold $\mathcal{M} \subset \mathbb{R}^2 \times \mathbb{R}^2 \times S^1$ can be defined by the product metric induced by the Riemannian distance on the object and finger surfaces as submanifolds of $\mathbb{R}^3$ and by the Riemannian distance on S^1 as a submanifold of $\mathbb{R}^2$ (namely, the distance in radians).

Kinematics of rolling can be derived from either the classical differential geometric viewpoint (using the first and second fundamental forms for a surface Σ, denoted as $\mathcal{I}$ and $\mathcal{II}$, respectively, and Christoffel symbols of the first and second kind, $[ij, k]$ and Γ^k_{ij}); or using Cartan's definitions of metric form M, curvature form K, and torsion form T. The relationship between the two sets of forms is given by $M = \sqrt{\mathcal{I}}$, $K = M^{-T}\,\mathcal{II}\,M^{-1}$, and $TM = M_{22}M_{11}^{-1}[\Gamma^2_{11}, \Gamma^2_{12}]$ (see e.g. [14], [10]. Observe that, at regular points for the parameterization, the coefficients of the metric and of the torsion tensors of the object surface are uniformly bounded and bounded away from zero.

According to the derivation of Montana [4], in the presence of friction (i.e., assuming a soft–finger contact model) one has $v = 0$, $\omega_z = 0$, and

$$\begin{aligned} \dot{x} &= M_f^{-1} K_r^{-1} w \\ \dot{u} &= M_o^{-1} R_\psi K_r^{-1} w \\ \dot{\psi} &= T_f M_f \dot{x} + T_o M_o \dot{u}; \end{aligned} \tag{1}$$

where $K_r = K_f + R_\psi K_o R_\psi$ is the relative curvature form,

$$R_\psi = \begin{bmatrix} \cos\psi & -\sin\psi \\ -\sin\psi & -\cos\psi \end{bmatrix} = R_\psi^{-1},$$

and

$$w \stackrel{def}{=} \begin{bmatrix} -\omega_y \\ \omega_x \end{bmatrix}.$$

When the finger's surface is a plane (such as is the case in the grippers considered in this paper), one has immediately $K_f = 0$ and $T_f = 0$, while the metric tensor M_f is the identity matrix. In this case, rolling equations reduce to

$$\begin{aligned} \dot{x} &= \bar{w} \\ \dot{u} &= M_o^{-1} R_\psi \bar{w} \\ \dot{\psi} &= T_o R_\psi \bar{w}, \end{aligned} \tag{2}$$

with $\bar{w} \stackrel{def}{=} R_\psi K_o^{-1} R_\psi w$, and hence have a strictly triangular structure, i.e. it is possible to solve the ordinary differential equation (2) by successive applications of time integrals (quadratures).

III. Exploration and Reconstruction of Unknown Objects

As already mentioned, parts to be manipulated are sometimes not known a priori to the robot, and information on their shape may need to be gathered before manipulation can be planned and executed. In this section we describe the means by which it is possible to elicit shape information from rolling, with particular reference to the case of regular surfaces.

A procedure to explore the surface of unknown objects can be simply devised as follows:

i) The hand (with fingers open) is put around the object to be explored, and then closed in guarded mode with a contact force threshold;

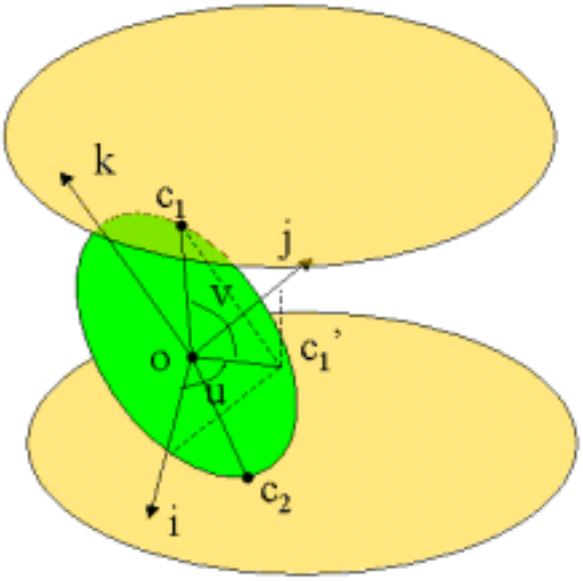

Fig. 1. Spherical coordinates on an object under roling manipulation for exploration.

ii) While actuators commanding the distance between the fingers regulate a suitable grasping force to avoid slippage, the actuators that command relative rotations and translations of the fingers follow random trajectories causing the object to roll between the fingers;
iii) the position of the contact point on the surface of the upper and lower fingers, as well as the position and velocity of the gripper joints, are measured during exploration; this information is used to calculate the position and velocity of the contact points on the object surface.

To reconstruct an approximation of the surface of the object, it is necessary to evaluate the instantaneous position of the contact points with respect to a cartesian frame fixed with the object. Let the origin of this frame be denoted by o, and let three unit vectors parallel to the x, y, and z axes of the body frame be denoted by i, j, and k, respectively (see fig.1). Let the object surface be described in spherical coordinates, i.e., the position of a generic point (except the north and south poles) of the surface in the body–fixed frame is given in terms of azimuth $u \in [-\pi, \pi)$ and elevation $v \in (-\pi/2, \pi/2)$ angles as

$$\begin{cases} x = \rho(u,v)\cos v \cos u \\ y = \rho(u,v)\cos v \sin u \\ z = \rho(u,v)\sin v \end{cases} \tag{3}$$

where $\rho(u,v)$ is a continuous function of the azimuth and elevation u, v. Notice that spherical coordinates are convenient for several reasons, among which is the fact that they provide an orthogonal parameterization of all surfaces of revolution (i.e., surfaces with an axis of symmetry), except at their poles. For surfaces of revolution, $\rho_u \stackrel{def}{=} \frac{\partial \rho(u,v)}{\partial u} = 0$. The position of the contact points on the upper and lower finger (denoted by c_1 and c_2, respectively) being known from tactile sensing, their velocities $\dot{c}_1$ and $\dot{c}_2$ with respect to a fixed wrist frame can be easily calculated by using the finger Jacobian matrix and measures of finger joint velocities. From data on the position and velocity of two points on the rigid object being manipulated, and using assumptions on friction at the contacts, one easily obtains the instantaneous angular velocity ω of the rolling object in the wrist frame.

The object motion is described by the following differential equations:

$$\begin{aligned} \dot{o} &= \dot{c}_1 + \omega \times (o - c_1) \\ \dot{R} &= \omega \times R \end{aligned}$$

Integrating these equations during the exploration time, the instantaneous position and orientation of the body can be obtained. From geometric considerations (see fig.1) we obtain at each time t the desired information on the coordinates of two points of the object surface from tactile sensor measurements $c_1(t)$ and $c_2(t)$ from (3) by setting for $i = 1, 2$

$$\begin{aligned} v_i(t) &= \arcsin \frac{(c_i - o)^T k}{\rho_i}; \\ u_i(t) &= \text{atan2}\ \left((c_i' - o)^T j,\ (c_i' - o)^T i\right); \\ \rho_i(t) &= \|c_i - o\|, \end{aligned}$$

where

$$c_i' = c_i - \rho_i \sin v_i k.$$

The problem of reconstructing a surface from knowledge of a number of its points is an important issue common to several fields of science and engineering. In robotics, the problem has been studied extensively in relation with processing data from cameras, range finders, and/or tactile sensors. Part of the literature is concerned with the "object recognition", or model matching problem (see e.g. [15], [16], [17], [18]). Works concerned with shape reconstruction deal with fitting experimental data with general models of surfaces (see e.g. [19], [20]). Various methods are distinguished by the information used and the surface model adopted to fit data. Allen [21] used bicubic (Coons') patches to fit data from vision and touch sensors, while [22] used superquadrics; [23] approximated objects by surfaces of revolution, and were able to determine their axis of symmetry by using tactile measurement of contact points, contact normals, and curvatures at the contact points; [24] considered haptic recognition of objects based on polyhedral shape approximations.

With respect to the existing literature, where surface reconstruction is mostly intended for object recognition, the problem we consider is to gather the surface information necessary to obtain sufficiently accurate formulae for the control vector fields appearing in the differential equation of rolling (2). As these vector fields are computed through differential operations from the surface description, it is necessary not only that the reconstruction is given in terms of analytic functions which are defined on as large a domain

as possible, but also are sufficiently smooth to avoid noise amplification through differentiation.

In order to master completely the accuracy/smoothness tradeoff in reconstruction, we found tools from regularization theory to be most effective (see e.g. [25] and [26]). In that framework, the problem of finding the "best" function approximating a multivariate function $y(x)$, whose values y_i at k points x_i are known (although with errors), is formulated as the minimization of the variational expression

$$H(f) = \sum_{i=0}^{k} (y_i - f(x_i))^2 + \lambda \|Pf\|^2 \tag{4}$$

where P is a differential operator used to weigh the "bumpiness" of the approximating function, and λ is a regularization parameter, that controls the compromise between the degree of smoothness of the solution, and its closeness to data ([27]). Such standard regularization technique provides solutions that are equivalent to generalized splines: for example, for single variable functions, it can be shown that with the differential operator

$$\|Pf\|^2 = \int_R \left[\frac{\partial^2 f(x)}{\partial x^2} \right]^2 \partial x$$

the solution of the regularization problem is given by cubic splines. In general, solution of (4) leads to the associated Euler-Lagrange equation

$$\hat{P}Pf(x) = \frac{1}{\lambda} \sum_{i=0}^{k} (y_i - f(x))\delta(x - x_i) \tag{5}$$

where $\hat{P}$ is the adjoint operator of P and δ is the Dirac delta function. The solution of (5) can be written as

$$f(x) = \frac{1}{\lambda} \sum_{i=0}^{k} (y_i - f(x_i))G(x; x_i) \tag{6}$$

where $G(x; x_i)$ are the Green functions of the differential operator $\hat{P}P$. Green functions are actually *radial* functions of their arguments $G(x; y) = G(\|x - y\|)$ when P is rotationally and translationally invariant. In such case, the solution of the regularization problem is a sum of *radial basis functions*:

$$f(x) = \sum_{i=0}^{k} c_i G(\|x - x_i\|), \tag{7}$$

where the weights c_i can be evaluated by simple linear algebraic operations. Some commonly encountered radial basis functions used in regularization theory and in the closely allied field of neural networks are

$$G(r) = \begin{cases} r & \text{(linear interpolation)} \\ r^3 & \text{(cubic interpolation)} \\ \sqrt{r^2 + c^2} & \text{(multiquadric)} \\ \frac{1}{\sqrt{r^2 + c^2}} & \text{(inverse multiquadric)} \\ e^{-\frac{r^2}{\sigma^2}} & \text{(gaussian)} \end{cases}$$

The problem of reconstructing a surface described in spherical coordinates (3) amounts to approximating a smooth function $\rho : S^2 \to \mathbb{R}$, $\rho = \rho(u, v)$ of the azimuth and elevation angles u, v, for which a set of points $\rho(u_i, v_i) = \rho_i$ are given from exploration data. With respect to the theory above resumed, the fact that the domain manifold S^2 is not globally equivalent to $\mathbb{R}^2$ imposes some modifications in the choice of basis functions. Following [26], we choose

$$\rho = \sum_{l=0}^{n} \sum_{s=-l}^{l} f_{ls} Y_{ls} \tag{8}$$

where f_{ls} are coefficients, and Y_{ls} are the eigenfunctions of the (surface) Laplacian on the sphere, i.e. the *spherical harmonics*, whose expression in coordinates is

$$Y_{ls}(u, v) = \begin{cases} U_{ls} \cos(us) P_l^s(\sin v) & 0 < s \le l \\ U_{ls} \sin(us) P_l^{|s|}(\sin v) & -l \le s < 0 \\ U_{l0} P_l(\sin v) & s = 0 \end{cases} \tag{9}$$

for $l = 0, 1, \ldots$. Here,

$$\begin{aligned} U_{ls} &= \sqrt{2} \sqrt{\tfrac{2l+1}{4\pi} \tfrac{(l-|s|)!}{(l+|s|)!}} && s \neq 0 \\ &= \sqrt{\tfrac{2l+1}{4\pi}} && s = 0 \end{aligned}$$

P_l, $l = 0, 1, \ldots$, are the Legendre polynomials, and P_l^s are the Legendre functions

$$P_l^s(z) = (-1)^s (1 - z^2)^{\frac{s}{2}} \frac{\partial^s}{\partial z^s} P_l(z)$$

Notice that Y_{l0} are surfaces of revolution. The unknown coefficients are obtained by minimizing the regularized spherical least–squares functional

$$\begin{aligned} H(\lambda) &= \frac{1}{n} \sum_{i=1}^{k} \left(\rho_i - \textstyle\sum_{l=0}^{n} \sum_{s=-l}^{l} f_{ls} Y_{ls}(u_i, v_i) \right)^2 \\ &\quad + \lambda \sum_{l=0}^{n} \sum_{s=-l}^{l} [l(l+1)]^m f_{ls}^2 \end{aligned} \tag{10}$$

Arranging the index set $\{(l, s)\}$ in a convenient order, and letting f be the vector of f_{ls} and X be the matrix with $(i, ls)_{th}$ entry $Y_{ls}(u_i, v_i)$, (10) becomes

$$\frac{1}{n} \|y - Xf\|^2 + \lambda f^T D f$$

where D is the diagonal matrix with $(ls, ls)_{th}$ entry $[l(l+1)]^m$. The minimizing vector f_λ is simply obtained by solving the following linear system of equations,

$$f_\lambda = (X^T X + \lambda D)^{-1} X^T y.$$

IV. Planning Rolling Manipulation

In this section we describe a technique for planning manipulation by rolling for general objects. Previous methods proposed to this purpose include techniques for particular

cases (typically, for a rolling sphere, see e.g. [7]), and very general iterative methods such as the generic loops method of Sontag [28], or the continuation method of Sussmann and Chitour [29]. A technique was proposed in [10] which effectively reduced the problem of planning for general surfaces to the solution of a system of two nonlinear algebraic equations in two unknowns.

All the above methods share two intrinsic limitations. Firstly they are, in one guise or another, iterative methods whose convergence rate is typically slow and hard to predict (no general exact planning method is known at the state of the art). Secondly, they do not consider the possible presence of obstacles. Planning among obstacles is a crucial problem in our application, because joint limits and physical boundaries of the manipulating surfaces impose constraints on the configuration space.

The problem of planning for nonholonomic systems among obstacles was attacked by [30] with an iterative method derived from those of [28], [29]. A general approach to the problem was considered by [31], who introduced a general topological property of exact planning algorithms in free space, capable of guaranteeing their applicability to planning problems in constrained spaces.

Our aim in this section is to devise a planning algorithm for rolling manipulation that i) can guarantee convergence to within a given tolerance of the desired final configurations in a finite and predictable number of steps, and ii) can be applied in the presence of constraints in the configuration space.

The basic ingredient of the planner we propose is a lattice structure we superimpose to the configuration space of the rolling system. The lattice, whose mesh size can be adjusted to suit the required accuracy, is obtained by choosing a finite number of basic actions (which could be regarded as control "atoms" or "quanta") to be taken on the system, and considering the effects on the system of applying all the (countably infinite) possible different sequences of such actions. The problem of steering on this lattice will then be solved by constructing a suitable sequence of control quanta. This technique was inspired by similarity with the solution obtained to the planning problem for rolling polyhedral parts, where the quantized nature of control inputs is intrinsic (see [32], [12]).

The rest of this section is organized as follows: in IV-A we slightly generalize the definition of the topological property of [31] to approximate planning algorithms, and discuss its applications to nonholonomic systems in constrained configuration spaces. In IV-B we describe the general structure of our proposed algorithm; IV-C introduces the basic geometric construction underpinning the algorithm, and IV-D contains the proof of the fact that the proposed algorithm indeed has the invoked topological property.

A. Planning nonholonomic systems among obstacles

Consider the problem of steering a nonholonomic system on a manifold $\mathcal{M}$ between two configurations $p_0, p_{goal} \in \mathcal{M}$, through a trajectory which is admissible with respect to both restrictions on the workspace and nonholonomic constraints. A possible approach is to find first a solution to the (much simpler) problem obtained by removing the nonholonomic constraints, and then to find an approximation to that solution that satisfies the nonholonomic constraint, while keeping away from obstacles.

Assume that the initial and final configurations belong to the same connected component of the free configuration space $\mathcal{C}_{free}$, which is assumed to be an open set. Assume further that a trajectory (or *geometric path*) $\gamma : [0,1] \mapsto \mathcal{M}$, $\gamma(0) = p_0$, $\gamma(1) = p_{goal}$ results from a global planner, such that $\gamma(t) \in \mathcal{C}_{free}$, $t \in [0,1]$. The approximating nonholonomic path Γ is in general comprised of a finite concatenation of subpaths

$$\Gamma_i : [0,1] \mapsto \mathcal{M},\ i = 1, \ldots, N,$$

where $\Gamma_i(1) = \Gamma_{i+1}(0)$, $\Gamma_1(0) = p_0$ and $\Gamma_i(1) \in V(p_i)$ with $V(p_i)$ a neighborhood of a point p_i on γ. We do not insist here that the approximating local planner is exact, because such property is not enjoyed by any known planner for rolling motion. However, for all i we assume that the local planner output Γ_i is

- feasible with respect to the nonholonomic constraints, and
- *local–local*, i.e. if the initial and final points of Γ_i are close enough, then Γ_i does not exit a small neighborhood of the initial point.

Denoting by $B(p, \epsilon)$ a ball centered in p of radius ϵ, a more precise definition of the latter property is as follows:

Definition 1: A local planning algorithm is *local–local* if for any initial configuration p_0 and for all neighborhoods $U(p_0)$ of p_0, there exists a *locally reachable neighborhood* $R(p_0) \subset U(p_0)$ such that, for any goal configuration $p_1 \in R(p_0)$ and for all $\varepsilon > 0$, the algorithm provides a trajectory $\hat{\Gamma} : [0,1] \mapsto \mathcal{M}$ steering the system from $p_0 = \hat{\Gamma}(0)$ to $\tilde{p}_1 = \hat{\Gamma}(1) \in B(p_1, \varepsilon)$ with $\hat{\Gamma}(t) \in U(p_0)\ \forall t \in [0,1]$.

Such local–local property is clearly a relaxed version of the "topological property" introduced by [31] for exact local planners.

Let a tubular neighborhood τ of the geometric path γ be defined as

$$\tau = \cup_{p \in \gamma} U(p)$$

with $U(p) = B(p, \epsilon(p))$, with $\epsilon(p)$ bounded away from zero (i.e., $\epsilon(p) \geq \epsilon > 0, \forall p \in \gamma$), and assume that $\tau \subset \mathcal{C}_{free}$. Under the assumptions above, a nonholonomic path Γ in the free configuration space can be computed by iteratively applying a local–local algorithm as follows (see fig.IV-A):

1. Denote $U(p_0) \subset \tau$ a neighborhood of p_0 entirely contained in the free configuration space, and let $R(p_0)$ be the corresponding local reachability neighborhood of definition 1;

2. Choose $p_1 = \gamma(t)$ with $t = \max\{s :\ B(\gamma(s), \varepsilon) \subset R(p_0)\}$ and compute $\Gamma_1 : p_0 \mapsto \tilde{p}_1$ with $\tilde{p}_1 \in B(p_1, \varepsilon)$ and $\Gamma_1(t) \in U(p_0)\ \forall t \in [0,1]$;

3. For all $j \geq 2$, denote $U(\tilde{p}_{j-1}) \subset \tau$ a neighborhood of $\tilde{p}_{j-1}$ and $R(\tilde{p}_{j-1})$ the associated local reachability neighborhood. Choose $p_j = \gamma(t)$ with $t = \max\{s :\ B(\gamma(s), \varepsilon) \subset$

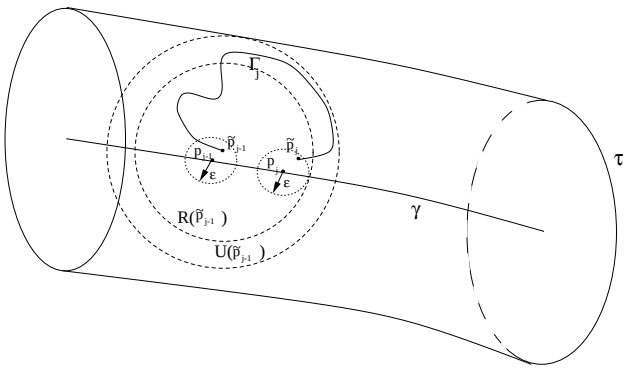

Fig. 2. Iterative application of a local–local planner provides an approximation of a geometric path that verifies both nonholonomic and configuration–space constraints.

$R(\tilde{p}_{j-1})\}$ and compute $\Gamma_j : \tilde{p}_{j-1} \mapsto \tilde{p}_j$ with $\tilde{p}_j \in B(p_j, \varepsilon)$ and $\Gamma_j(t) \in U(\tilde{p}_{j-1})\ \forall t \in [0,1]$.

Observe that the procedure above terminates if γ is such that there exists $\delta > 0$ such that $\inf\{\ \mathsf{diam}\ (R(p)),\ p \in B(\gamma, \delta)\} = \bar{\varepsilon} > 0$. If this is the case the variable ε of the algorithm must be smaller than $\bar{\varepsilon}$.

B. A local-local planner for rolling manipulation

We consider planning motions of an object of general, regular shape on a planar finger, as described by (2). Let $d(\cdot,\cdot)$ denote the distance between points $p = (u, x, \psi)$ in the state manifold for our problem $\mathcal{M} = \mathbb{R}^2 \times \mathbb{R}^2 \times S^1$ defined in section II.

Set $p_0 = (u_0, x_0, \psi_0) \in \mathcal{M}$ and $p_{goal} = (u_{goal}, x_{goal}, \psi_{goal}) \in B(p_0, \bar{\delta}_{\mathcal{M}})$, with $\bar{\delta}_{\mathcal{M}} \in \mathbb{R}$ a (small) positive number.

We propose to steer approximately the system between p_0 and p_{goal} through the following intermediate steps:

$$p_0 \overset{Step1}{\mapsto} p_a = (u_{goal}, x_a, \psi_a)$$

$$p_a \overset{Step2}{\mapsto} p_b = (u_{goal}, x_b, \tilde{\psi}_{goal})$$

$$p_b \overset{Step3}{\mapsto} \tilde{p}_{goal} = (u_{goal}, \tilde{x}_{goal}, \tilde{\psi}_{goal})$$

with $\tilde{p}_{goal} \in B(p_{goal}, \varepsilon)$.

These steps will be described and analyzed in detail in the following. To substantiate our claim that the algorithm can steer a rolling body to an arbitrarily small neighborhood of the desired final configuration using a finite number of maneuvers and satisfying the local–local property, we need to introduce some further notation.

Denote

$$\delta_u, \delta_x, \delta_\psi \in \mathbb{R}, \quad \text{positive with } \delta_u^2 + \delta_x^2 + \delta_\psi^2 \leq \delta_{\mathcal{M}}^2, \quad (11)$$

$$\bar{\delta}_u, \bar{\delta}_x, \bar{\delta}_\psi \in \mathbb{R}, \quad \text{positive with } \bar{\delta}_u^2 + \bar{\delta}_x^2 + \bar{\delta}_\psi^2 \leq \bar{\delta}_{\mathcal{M}}^2 \quad (12)$$

and, finally,

$$\varepsilon_u^2, \varepsilon_x^2, \varepsilon_\psi^2 \in \mathbb{R}, \quad \text{positive with } \varepsilon_u^2 + \varepsilon_x^2 + \varepsilon_\psi^2 \leq \varepsilon_{\mathcal{M}}^2; \quad (13)$$

The local–local property of the algorithm will be proved by showing that the resulting trajectory $(u(t), x(t), \psi(t))$ is such that if $u_{goal} \in B(u_0, \bar{\delta}_u)$, $x_{goal} \in B(x_0, \bar{\delta}_x)$ and $\psi_{goal} \in B(\psi_0, \bar{\delta}_\psi)$, then $\forall t$, $u(t) \in B(u_0, \delta_u)$, $x(t) \in B(x_0, \delta_x)$ and $\psi(t) \in B(\psi_0, \delta_\psi)$ with

$$(\delta_u, \delta_x, \delta_\psi) \mapsto 0 \ \text{ for } (\bar{\delta}_u, \bar{\delta}_x, \bar{\delta}_\psi) \mapsto 0. \quad (14)$$

Step 1 The first step consists simply in applying to system (2) a constant control $\bar{w}(t) = \bar{w}_a$, $0 \leq t \leq t_a$ such that $u_0 \mapsto u(t_a) = u_{goal}$ exactly. The corresponding trajectory on the plane is a straight line and its length is equal to the Riemannian distance on the surface between u_0 and u_{goal}. Then if $d(u_0, u_{goal}) \leq \bar{\delta}_u$ we set $\delta_u = \delta_x = \bar{\delta}_u$. By geometric analysis of the system equations (see e.g. [10], the infinitesimal variation ψ is equal to the infinitesimal variation of the angle between the coordinate direction of the object surface and the tangent to the curve. Then in a small neighborhood of u_0 the total variation of $\psi(t)$ is bounded and this bound decreases to zero with $\bar{\delta}_u$.

Step 2 Consider the set $\mathcal{L}$ of closed, simple paths of length ϱ on the object surface. Let θ denote the direction of the curve at the initial point u_{goal} in the reference frame of the plane of the finger. Recall that rolling an object on a plane along a closed path on the object surface produces a change in the final orientation of the object which is given by the holonomy angle, i.e. the integral of the gaussian curvature comprised in the portion of region bounded by the curve. In the following subsection (IV-C) a particularly useful subset $\mathcal{R} \subset \mathcal{L}$ will be introduced, from which an element corresponding to a pair $(\bar{\theta}, \bar{\varrho})$ can be chosen such that the corresponding holonomy angle $\Delta\psi \leq \frac{\varepsilon_\psi}{2}$. Then there exists an integer N (the integer part of $\frac{|\psi_a - \psi_{goal}|}{\Delta\psi}$) such that $\|\psi_a + N\Delta\psi - \psi_{goal}\| \leq \varepsilon_\psi$ and the corresponding closed path $(\bar{\theta}, \bar{\varrho})$ applied N times steers the system in a configuration $p_b = (u_{goal}, x_b, \tilde{\psi}_{goal})$ with $\tilde{\psi}_{goal} = \psi_a + N\Delta\psi \in B(\psi_{goal}, \varepsilon_\psi)$. The proof of the local–local property of this trajectory is postponed to subsection IV-D.

Step 3 By this step, the system is steered to some configuration $(u_{goal}, \tilde{x}_{goal}, \tilde{\psi}_{goal})$ with $\|\tilde{x}_{goal} - x_{goal}\| \leq \varepsilon_x$ by applying the following method: observe that $\mathcal{L}$ is a subgroup of the fundamental group of closed paths with base point u_{goal}, i.e. $\mathcal{L}$ is closed under concatenation and inverse. Consider the map Ξ:

$$\Xi : \mathcal{L} \longrightarrow \mathbb{R}^2 \times S^1$$

where $\Xi(l) = (v, \Delta\psi)$, where v denotes the total translation of the contact point on the plane, and $\Delta\psi$ is the net change in the orientation of the object that are obtained corresponding to applying to the rolling object a motion that makes the contact point on the object follow a closed path (i.e., an element of $\mathcal{L}$). For this map Ξ the following properties hold:

a) let l_1 and l_2 be any two paths in $\mathcal{L}$ with $\Xi(l_1) = (v_1, \Delta\psi_1)$ and $\Xi(l_2) = (v_2, \Delta\psi_2)$, then for their concatenation we have (in exponential notation)

$$\Xi(l_2 \circ l_1) = (v_2 e^{i\Delta\psi_1} + v_1, \Delta\psi_2 + \Delta\psi_1).$$

The first component of $\Xi(l_2 \circ l_1)$ is the sum of two vectors of $\mathbb{R}^2$ taking into account that the orientation of the reference frame on the tangent plane at contact point u_{goal} has changed by $\Delta\psi_1$ after that the execution of l_1 is completed. The second component denote the total change of orientation produced by the two paths.
b) As the length l of the path goes to zero, $\Xi(l) \mapsto (0,0)$. Indeed, Ξ describes the end point map of a smooth differential system with piecewise continuous input, for which continuity of solutions is given by classical results.

Now, consider the existence of closed paths $l \in \mathcal{L}$ that achieve translations of the object on the plane, without changing its orientations, or in other terms, such that

$$\Xi(l) = (v, 0). \tag{15}$$

By the composition law given above, it is clear that such paths exist: indeed, for instance, any element of the commutator subgroup of $\mathcal{L}$ defined as

$$[\mathcal{L}] = \{[l_1, l_2] = l_1^{-1} \circ l_2^{-1} \circ l_1 \circ l_2,\ l_1, l_2 \in \mathcal{L}\}$$

satisfies equation 15. Let $\widehat{\mathcal{L}} \subset \mathcal{L}$ denote the set of such paths, and consider a finite subset $\{\hat{l}_i, i = 1, M\}$, each corresponding to a pure translation of the object in the plane by a quantity $\hat{v}_i \in \mathbb{R}^2$. By concatenating (in arbitrary order) such paths taken an integer number of times, i.e. $\alpha_1\hat{l}_1 \circ \alpha_2\hat{l}_2 \circ \cdots \alpha_M\hat{l}_M$, $\alpha_i \in \mathbb{Z}$, a net translation of the object is obtained that is given by

$$\hat{v}(\alpha) = \alpha_1\hat{v}_1 \circ \alpha_2\hat{v}_2 \circ \cdots \alpha_M\hat{v}_M \tag{16}$$

In other words, the object can be translated by any integer combination of the 2-vectors $\hat{v}_i$, that play the role of control quanta in our planning scheme. It is well known from the theory of linear integer programming, that the set of achievable translations resulting from (16) is a lattice of points in the plane[1].

Such lattice can be made arbitrarily fine. Indeed, assume (it will be proved in section IV-C) that there exist paths $l_i^j \in \mathcal{L}$, $i = a, b$, $j = 1, 2$ such that

$$\|\Xi(l_i^j)_1 = v_i^j\| \leq \varepsilon_x \ i = a, b, j = 1, 2 \tag{17}$$

Then, paths $\hat{l}_i = [l_i^1, l_i^2] \in \widehat{\mathcal{L}}$, $i = a, b$ are such that $\max\{\frac{\|\hat{v}_a - \hat{v}_b\|}{2}, \frac{\|\hat{v}_a + \hat{v}_b\|}{2}\} \leq \varepsilon_x$.

In conclusion, a suitable linear integer combination of elementary paths $\hat{l}_i$ can be easily found (by standard ILP techniques such as Hermite normal forms, see e.g. [33]) that steers the system to some configuration $(u_{goal}, \tilde{x}_{goal}, \tilde{\psi}_{goal})$ with $\|\tilde{x}_{goal} - x_{goal}\| \leq \varepsilon_x$. A bound on the number of elementary paths that guarantee convergence to within the desired tolerance can be provided (see [11] where the same techniques are used in planning for polyhedral objects). The local–local property of this kind of trajectories will be shown in Section IV-D.

[1] we assume that all $\hat{v}_i$ have rational components

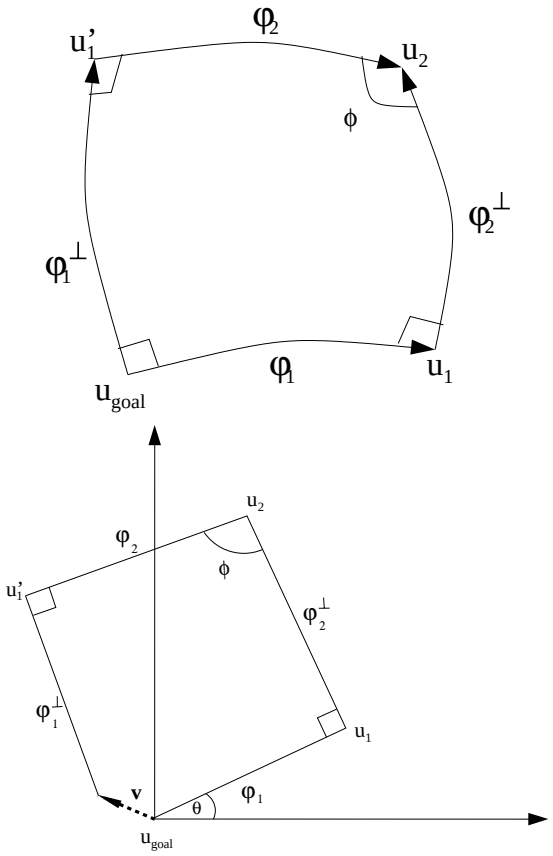

Fig. 3. The geometric construction of a geodesic rectangle (top) and its trace on the plane (bottom)

C. Geodesic Quadrilaterals

A particular class of closed paths can be used such that the geometrical properties of the system are exploited and the resulting trajectories can be easily computed. Closed paths on the object's surface that are comprised of segments of geodesic curves have the following very useful properties:

- the corresponding trajectory on the finger is piecewise linear. Indeed, if the contact point traces a geodesic curve on one surface of a rolling pair, then it also traces a geodesic on the second surface (see e.g. [34]). On the flat finger surface, geodesics are straight lines;
- each linear segment of the trajectory on the finger has the same length as the corresponding geodesic segment on the object surface; the angle between adjacent segments is the same on the two surfaces;
- by the Gauss-Bonnet theorem, the total change in the holonomy angle ψ due to a piecewise geodesic path correspond to the defect to 2π of the sum of the angles between adjacent geodesic segments.

Consider then a *geodesic quadrilateral* $R(\theta, \varrho)$ comprised of four segments of geodesics on the object's surface. The first point chosen for the construction is the base point u_{goal} (i.e., the desired point of contact on the object surface reached after the first step of the proposed algorithm).

Recall that the object surface is parametrized by $f : \mathbb{R}^2 \mapsto \mathbb{R}^3$. A geodesic quadrilateral $R(\theta, \varrho)$ of *size* $\varrho \in \mathbb{R}$

and *orientation* $\theta \in S^1$ is built as follows (see fig. 3):
1. let $\varphi_1(s)$ be a geodesic curve such that

$$\varphi_1(0) = u_{goal} \quad \text{and} \quad \frac{\dot\varphi_1(0)}{\|\dot\varphi_1(0)\|}^T \frac{\hat{f_u}}{\|f_u\|} = \cos\theta;$$

2. let $\varphi_1^\perp(s)$ a geodesic curve such that

$$\varphi_1^\perp(0) = u_{goal} \quad \text{and} \quad \frac{\dot\varphi_1^\perp(0)}{\|\dot\varphi_1^\perp(0)\|}^T \frac{\dot\varphi_1(0)}{\|\dot\varphi_1(0)\|} = 0;$$

3. let $\varphi_1(t_1) = u_1$ and $\varphi_1^\perp(t_1') = u_1'$ be two points on the surface such that their Riemannian distance from u_{goal} is ϱ;
4. let $\varphi_2(s)$ a geodesic curve such that

$$\varphi_2(0) = u_1' \quad \text{and} \quad \frac{\dot\varphi_1^\perp(t_1')}{\|\dot\varphi_1^\perp(t_1')\|}^T \frac{\dot\varphi_2(0)}{\|\dot\varphi_2(0)\|} = 0;$$

5. let $\varphi_2^\perp(s)$ a geodesic curve such that

$$\varphi_2^\perp(0) = u_1 \quad \text{and} \quad \frac{\dot\varphi_1(t_1)}{\|\dot\varphi_1(t_1)\|}^T \frac{\dot\varphi_2^\perp(0)}{\|\dot\varphi_2^\perp(0)\|} = 0.$$

6. $\varphi_2^\perp$ and φ_2 intersect each other, at least for ϱ sufficiently small. Denote $\bar\varrho = \sup\{\varrho : \varphi_2^\perp \cap \varphi_2 \neq \emptyset\}$. Consider the point of intersection $u_2 = \varphi_2(t_2) = \varphi_2^\perp(t_2')$ between the two curves and let ϕ be the angle between the two curves at point u_2.

Finally, let $R(\theta, \varrho)$ be the geodesic quadrilateral joining points u_{goal}, u_1, u_2, u_1', u_{goal} through the geodesics φ_1, $\varphi_2^\perp$, φ_2, $\varphi_1^\perp$.

Observe that, for small enough ϱ, the point u_2 belongs to some neighborhood of u_{goal}. Moreover, the angle ϕ between $\varphi_2^\perp$ and φ_2 at u_2, $d(u_1, u_2)$ and $d(u_1', u_2)$ depend continuously on ϱ, in particular

$$\lim_{\varrho \mapsto 0} d(u_1, u_2) = \lim_{\varrho \mapsto 0} d(u_1', u_2) = 0 \tag{18}$$

and

$$\lim_{\varrho \mapsto 0} \phi = \frac{\pi}{2}. \tag{19}$$

Next we describe the trace of the geodesic quadrilateral $R(\theta, \varrho)$ on the plane (see fig.3, bottom), which is comprised of 4 straight segments of length $d(u_0, u_1) = \varrho, d(u_1, u_2), d(u_2, u_1')$ and $d(u_1', u_0) = \varrho$, respectively, and angle $\theta, \theta + \frac{\pi}{2}, \theta + \frac{3\pi}{2} - \phi$ and $\theta - \phi$.

Clearly, any geodesic quadrilateral is an element of the group $\mathcal{L}$ described in the previous section and, denoting $d(u_1, u_2) = \varrho_1$ and $d(u_2, u_1') = \varrho_1'$, we have that its action on the rolling object configuration $\Xi(R(\theta, \varrho)) = (v, \Delta\psi)$ is given by

$$v = e^{i\theta}\left(\varrho + \varrho_1 e^{i\frac{\pi}{2}} + \varrho_1' e^{i\frac{3\pi}{2} - \phi} + \varrho e^{-i\phi}\right), \tag{20}$$

and (using the Gauss-Bonnet theorem)

$$\Delta\psi = \left(3\frac{\pi}{2} + \phi\right) - 2\pi = -\frac{\pi}{2} + \phi. \tag{21}$$

D. Proof of the Local–Local Property Using Geodesic Quadrilaterals

First we show that the second step of the proposed algorithm verifies the local property. By equation (19) and (21) we can fix $\varrho \leq \bar\varrho$ such that $\Delta\psi \leq \frac{\varepsilon_\psi}{2}$. Then the trajectory u on the object surface is the geodesic quadrilateral $R(\varrho, \theta)$ repeated $N = \left[\frac{|\psi_1 - \psi_2|}{\Delta\psi}\right]$ times. Clearly $u \subset B(u_{goal}, \delta_u)$ with $\delta_u = C'\varrho$ for some constant C'. As to locality of Step 2 in the plane, observe first that $v \in \mathbb{R}^2$ with $\Xi(R(\varrho, \theta)) = (v, \Delta\psi)$ is such that

$$\|v\| \leq C\varrho^2 \tag{22}$$

for some constant C. Indeed from equation (20) we obtain $\|v\|^2 = (\varrho - \varrho_1' \sin\phi + \varrho\cos\phi)^2 + (\varrho_1 - \varrho_1'\cos\phi - \varrho\sin\phi)^2$ and, being $\phi = \frac{\pi}{2} + O(\varrho)$, $\frac{\varrho_1}{\varrho} = 1 + O(\varrho)$, and $\frac{\varrho_1'}{\varrho} = 1 + O(\varrho)$, we immediately obtain (22). Moreover, we have the following facts:
1.

$$\Delta\psi = \int_\Omega K du\, dv \geq K_{min}\varrho^2$$

where Ω is the region bounded by the geodesic quadrilateral and K and K_{min} are respectively the Gaussian curvature and the minimum of the Gaussian curvature in the closed region Ω, and
2. let $V = \sum_{n=0}^N v e^{in\Delta\psi}$ be the total displacement on the plane; then $\|V\| < N\|v\|$

From equation (22) it follows that

$$\|V\| \leq \frac{|\psi_1 - \psi_{goal}|}{\Delta\psi} C\varrho^2 \leq \frac{|\bar\delta_\psi|}{K_{min}\varrho^2} C\varrho^2 \leq \frac{|\bar\delta_\psi|}{K_{min}} C$$

Then we have that the trajectory x on the plane is such that $x \subset B(x_1, \delta_x)$ with $\delta_x = C\frac{|\bar\delta_\psi|}{K_{min}} = C'\bar\delta_\psi$, $C' = \frac{C}{K_{min}}$.

There remains to show that the local–local property also holds for the third step 3 of the proposed algorithm. To prove this, it is sufficient to find $\varrho \leq \bar\varrho$ such that $\Xi(R(\varrho, \theta))$ verifies equation (17). By equation (22) it is sufficient to choose $\varrho \leq \min\{C'\sqrt{\varepsilon_x}, \bar\varrho\}$, with C' some positive constant.

On the object surface the trajectory u is entirely contained in a neighborhood $B(u_{goal}, \delta_u)$ with $\delta_u = C'\varrho$ for some constant C'. Moreover, along the trajectory, by equation (19),

$$|\psi(t)| \leq |\Delta\psi_1| + \Delta\psi_2| = |\frac{\pi}{2} - \phi_1| + |\frac{\pi}{2} - \phi_2| = C'\varrho$$

for some constant C'. Then for the trajectory ψ of the orientation it holds $\psi \in B(\psi_{goal}, \delta_\psi)$ with $\delta_\psi = C'\varrho$.

Finally for the trajectory x on the plane, a suitable combination of l_1 and l_2 can be found such that $x \in B(x_2, \delta_x)$ with $\delta_x = \bar\delta_x$.

Finally, let C be a constant bigger than all the constants C' found above, then we have that the parameters of equation (11) which hold for the global trajectory through steps 1,2, and 3 are (see fig.4,fig.5 and fig.6) as follows:

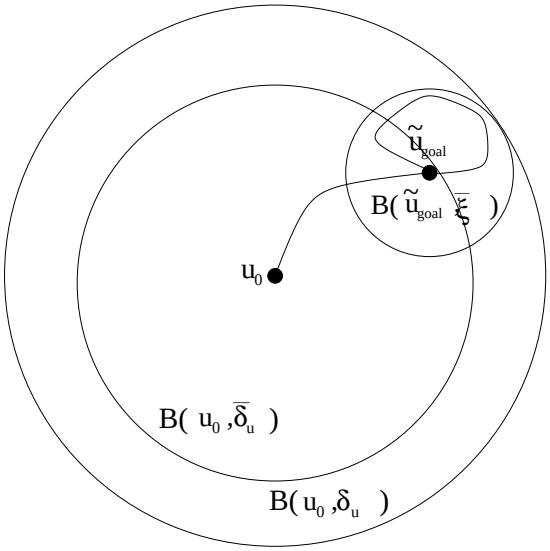

Fig. 4. The complete trajectory of the contact point on the object surface provided by the geodesic quadrilateral algorithm ($\bar{\zeta} = C\varrho_{min}$)

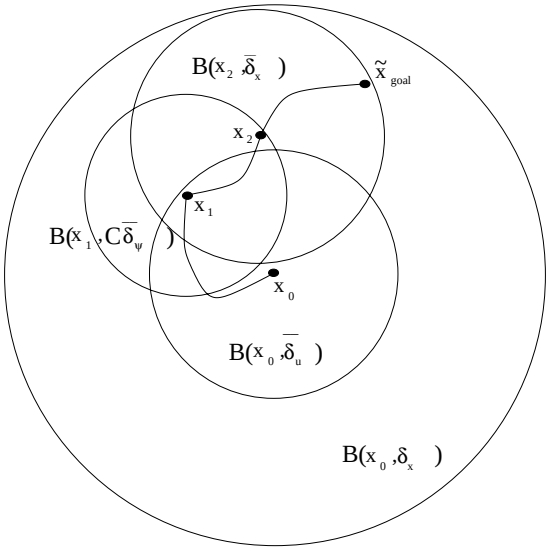

Fig. 6. The global trajectory of the contact point on the plane provided by the geodesic quadrilateral algorithm.

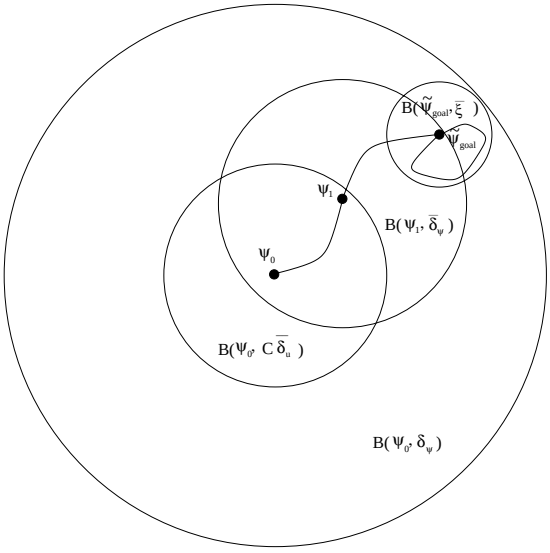

Fig. 5. The complete trajectory of the orientation provided by the geodesic quadrilateral algorithm (a two dimensional sketch is used for illustration,, although orientation is one-dimensional).

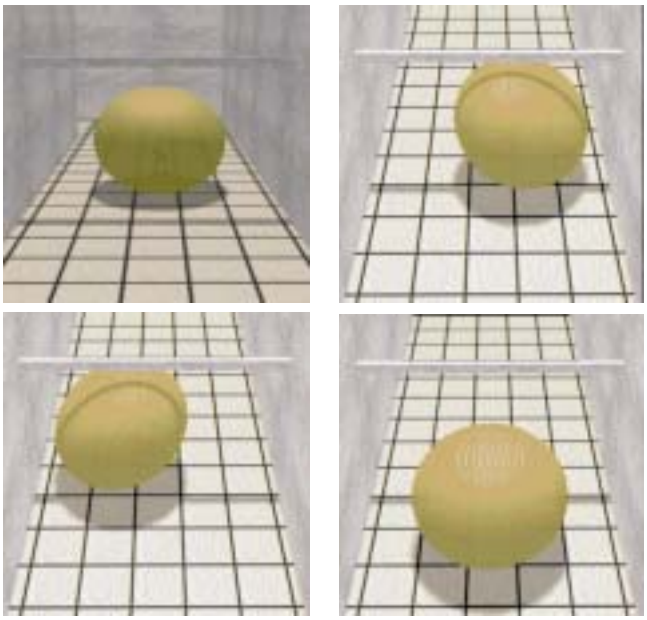

Fig. 7. Four frames of video in Multimedia Extension 1 (downloadable from ftp://131.114.28.35/pub/uploads)

$$\delta_u = \bar{\delta}_u + C\varrho_{min}$$
$$\delta_\psi = C\bar{\delta}_u + \bar{\delta}_\psi + C\varrho_{min}$$
$$\delta_x = \bar{\delta}_u + \bar{\delta}_x + C\bar{\delta}_\psi$$

where ϱ_{min} is the minimum among the parameters ϱ of Steps 1,2 and 3. Clearly any $\varrho \leq \varrho_{min}$ satisfy the local and steering properties of the algorithm and equation (14).

To illustrate the results of the above described algorithm, we report in Extension 1 (fig.7) the solution obtained for the problem of planning rolling motions for an ellipsoid (with principal axes of length 30, 30, and 20 cm) within a corridor of width 55 cm and height 25 cm. The solution to this rather complex planning problem was obtained on a Pentium-3 processor at 1.5 GHz in less than 1 minute, with an accuracy on the final configuration equal or better than 1% of the range of variation of each component. By reducing the required accuracy, faster calculation times can be achieved: however, such reduction is limited in this example, where the computational bottleneck is to find a path through the narrow passage among obstacles.

V. The Dextrous Gripper Dx-Grip-II

To experimentally validate the results of the theoretical work on manipulation by rolling conducted in the past years, the research group at Centro "E. Piaggio" of the University of Pisa designed and built two prototype end–

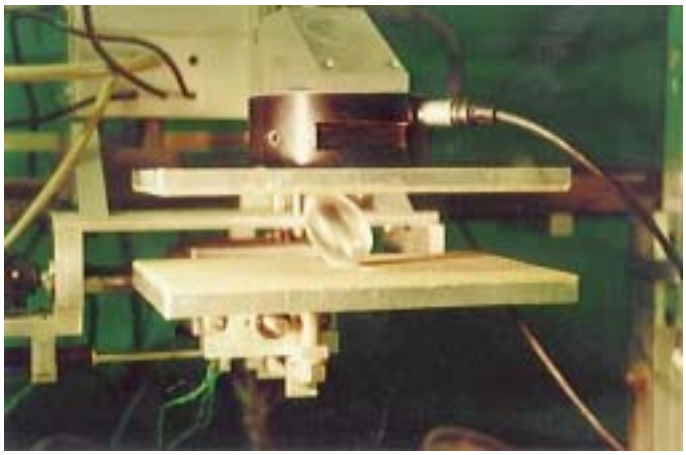

Fig. 8. The first University of Pisa Dextrous Gripper (DxGrip-I).

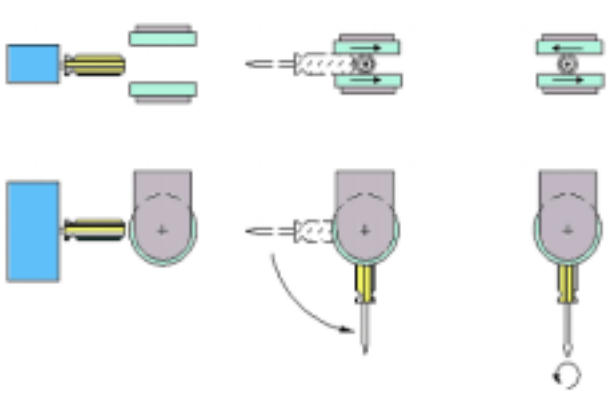

Fig. 10. Operation as a grasping and reorienting device

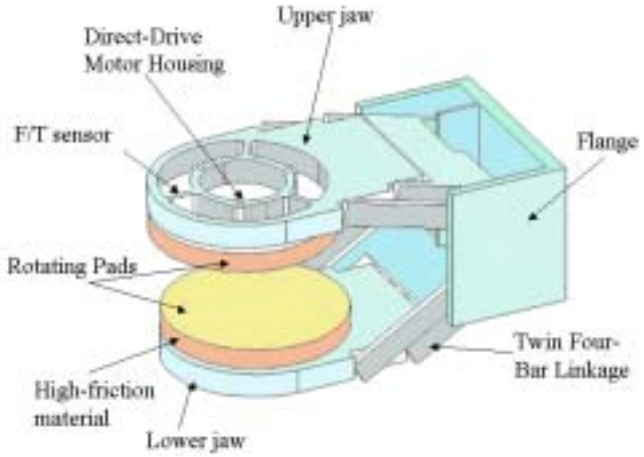

Fig. 9. Design of the second Dextrous Gripper of the University of Pisa, DxGrip-II.

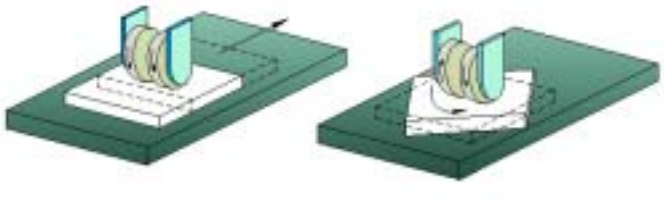

Fig. 11. Operation as a non–grasping manipulation device

effectors. The first "dextrous gripper", consisting of two parallel plates controlled by prismatic joints, was described in [8] (see fig.8). The gripper has two parallel planar jaws, of which the lower translates horizontally thus imparting rolling motions to the object, while the upper applies suitable grasping forces (measured by the force-torque sensor shown above the upper plate). Due to the kinematic decoupling among positioning and gripping d.o.f.'s, the operation of DxGrip-I was very simple and accurate. The gripper provided an excellent testbed for manipulation of both smooth and polyhedral surfaces, and has been employed for several experiments in the laboratory. However, some constructive features of DxGrip-I were not well adapted to building a robot gripper for genuine applications. In particular, the three lead-screw prismatic joints, two of which in cascaded arrangement for realizing the x-y movement for the lower jaw, made the overall design somewhat bulky and costly.

The main motivation to design a second generation dextrous gripper was to have a versatile device that could be considered as a viable substitution for current end-effectors at least in light-duty robotics applications. The design of DxGrip–II is described in fig.9. The gripper has two parallel jaws translating independently, and two turning disks on the jaws. Each jaw is driven by a DC minimotor (mounted within the gripper flange) through gears and a twin four–linkage mechanism, consisting of two four–bar linkages in quadrature. This mechanism eliminates singularities, so that the jaws can move smoothly across the configuration where the two legs shown in the figure are aligned. Each jaw has a rotating fingerpad actuated by miniature direct–drive brushless motors. These motors were built in our laboratory, by modifying existing motors designed for the spindles of high-performance computer disk–drives, for which the control logic and hardware were completely redesigned.

The hand has force/torque sensors on each fingerpad. Six–axis sensors are realized by strain–gages on the three flexures of a modified Maltese cross, to which the direct drive fingerpad actuators are fixed. By adding the measurements from the two jaw force/torque sensors, an equivalent wrist force/torque sensor is obtained. Intrinsic Tactile Sensing algorithms are used to elicit information on the location of the centroid of contact, the intensity and direction of contact force, the local torque, the risk of slippage, etc..

The low–level control of actuators is performed by a microcontroller (68HC11), with 512 bytes EEPROM and 512 bytes RAM, external 32K RAM and 32K EPROM. The microcontroller is connected to a host PC via fast RS232.

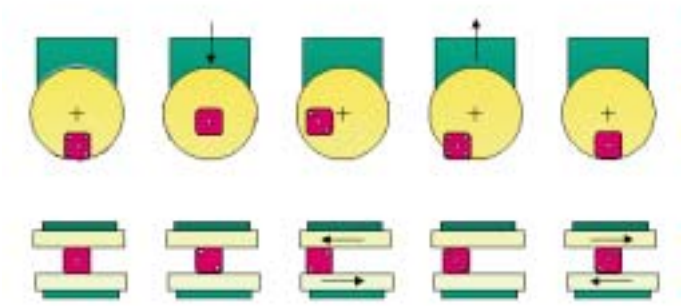

Fig. 12. Operation as a dextrous manipulator by rolling the object

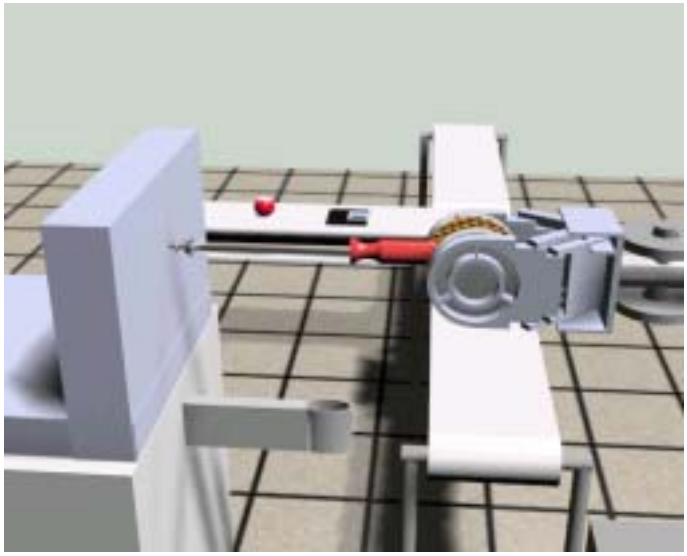

Fig. 13. First frame of video in Multimedia Extension 2 (downloadable from ftp://131.114.28.35/pub/uploads)

Fig. 14. Photographs of DxGrip-II showing the dimensions and the kinematic arrangement.

The microcontroller counts encoders, closes position control loops on the motors, reads A/D converters, manages timing, interrupts and communication with the host computer. The host computer evaluates forces/torques from sensor readings, computes intrinsic tactile sensing, plans and controls the kinematics of motion of the gripper.

As a consequence of the kinematic arrangement of DxGrip-II, the distance between the jaw planes can be changed independently from the distance between the axes of the revolving fingerpads, while the jaws always keep their parallel orientation. While the distance d.o.f. is used to control the grasping force so as to avoid slippage, the relative translation can generate a torque about an axis parallel to the plates, capable of inducing rolling in manipulated objects. Rolling along a perpendicular axis in the same plane can be obtained by combination of rotatory motions of the two plates. To generate such rolling torques and accomodate for the necessary compliance, fingerpads are covered with compliant, high friction material.

A seemingly difficult question arises in precisely modeling the frictional behavior of contacts. In particular, if both contacts were assumed to be of "soft-finger" type ([3]), i.e. preventing any spinning about the normal axis to the plates, then only motions with zero relative angular velocity of the two plates would be allowed. On the other hand, if both contacts are modeled as "hard-fingers", an indeterminacy of motion would ensue (rotations about an axis through the two contact points would result unconstrained). However, careful consideration of manipulation experiments naturally leads to easy solutions of this difficulty. A first possible solution is to consider a hard-finger model for both contacts, and impose that no rotations are allowed along the mentioned axis through contact points. According to this model, a spinning component ω_z of the angular velocity (perpendicular to the plate) would be present in general at the contacts: this effect could be taken into account (and compensated for) by considering corresponding terms in the rolling equations ([4]). In practice, however, we have found that by simply preparing the two fingerpads so that one has slightly lower friction than the other, the actual phenomenon is very well modeled by assuming a soft finger contact on one pad, and a hard-finger contact on the second.

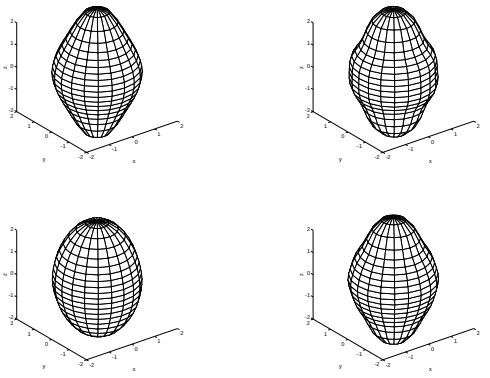

Fig. 15. Exact description of the manipulated object (upper left), and approximations with $\lambda = 0,002$ and $N = 7$ harmonics (underdamped, upper right), with $\lambda = 0,05$ and $N = 9$ (overdamped, lower left), and with $\lambda = 0,002$ and $N = 9$ (lower right).

The dextrous gripper has several modes of operation:
A) As a conventional parallel–jaw gripper, with the possibility of changing the grasp center–point in one direction. Wrist–force sensing and contact and friction sensing on the jaws is available through the combination of information from the finger force sensors.
B) As a reorienting device for grasped objects. Elongated objects such as tool handles can be rotated about the fingerpad axes and/or about their own axis, by combining equal or opposite angular velocities of the rotating fingerpads (see fig.10).
C) As a non–grasping manipulating device. The external cylindrical part of the fingerpads' surface can be pressed on flat parts lying e.g. on a conveyor belt, and manipulate them in the plane by translations and/or rotations, by combining equal or opposite angular velocities of the rotating fingerpads (see fig.11).
D) As a dextrous manipulator, capable of arbitrarily displacing and reorienting a manipulated object by rolling it between the fingerpads. This manipulation feature exploits the above mentioned results on nonholonomic systems planning and control, showing that practically any object (including objects bounded by polyhedral hulls) can be arbitrarily manipulated in 3D space by suitably combining the d.o.f.'s of the dextrous gripper (see fig.12).
A pictorial animation of DxGrip-2 used in a variety of tasks is reported in Extension 2 (fig.13). Two pictures of a prototype version of DxGrip-II are reported in fig.14. It should be pointed out that, while the use of turntables at the fingers of a gripper has already been proposed by Nagata [35], DxGrip–II has the possibility of translating the center of one turntable with respect to the other, thus achieving higher dexterity and most importantly the ability of rolling an object in all directions between the fingers.

A. Experimental Results

Experiments to assess the performance of the proposed exploration and reconstruction procedure have been performed using the hardware described above. The force sensors on the gripper jaws are used to control the grasping force and avoid slippage. To detect the location of contact points on the upper and lower fingers, the same sensors can be used in conjunction with the "intrinsic" tactile sensing algorithms described in [36].

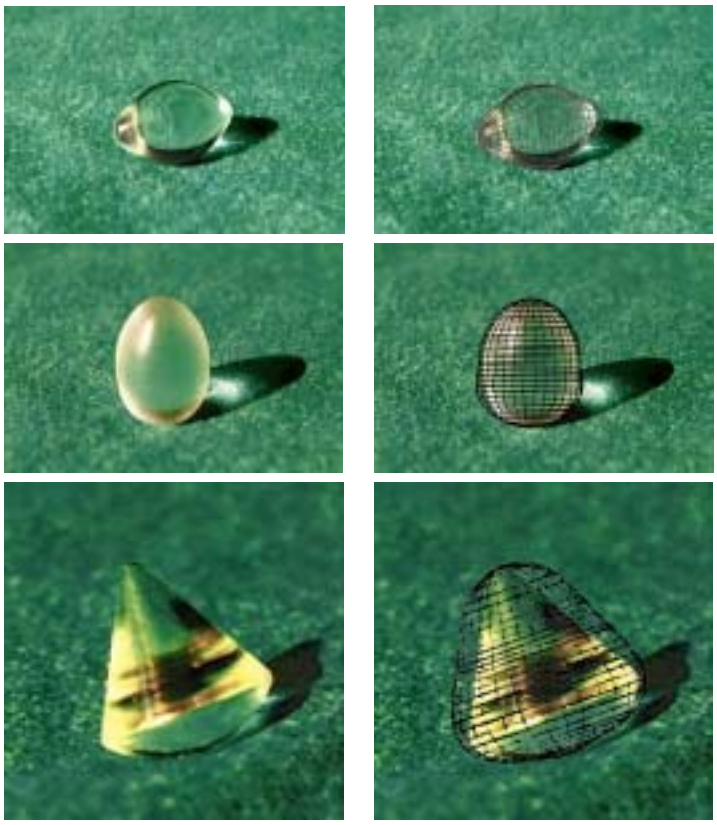

Fig. 16. Three objects and their reconstruction from experimental data gathered by rolling manipulation.

Figure fig.15 shows the effects of various parameters in the reconstruction algorithm. Apparently, using few spherical harmonics (low N) and/or low regularization weights λ provides "bumpy" reconstructions, while heavy regularization tends to round up the object shape excessively. The correct tradeoff in filtering has to be decided on the basis of a working knowledge of the sensor noise statistics and of the application domain. Experimental reconstructions of three different objects are reported in fig.16. The third object, whose surface is obtained by intersecting a cone with a sphere, poses a challenging problem to approximation, as the nominal surface contains the whole spectrum of spatial frequencies, from zero (along the cone generatrices, where the gaussian curvature is zero) to infinity (at the cone vertex). In general, the reconstruction accuracy is probably less than what could be obtained by other means, such as e.g. optical. However, we consider the obtained results to be quite satisfactory, in view of the following facts:

- the procedure uses only (noisy) force sensors, but could be easily integrated with other data (a priori known, or from optical sensors);
- shape reconstruction is done while manipulation proceeds, and not in a preliminary calibration phase;
- a mathematical description of the object is obtained,

which is globally valid and everywhere smooth on the object's surface. This is an important point to allow the application of manipulation planning algorithms. The necessary degree of regularity of the mathematical model to be used in planning inherently conflicts with accuracy, and forces to "smooth out" vertices of the reconstruction (see e.g. the third object in fig.16). Other reconstruction approaches, based on local approximations of the surface (such as those used in CAD and computer graphics), might achieve a better accuracy pointwise, but would be unsuitable to the planning phase.

VI. Discussion and Conclusion

In this paper we have considered some of the problems that hinder the practical implementation of dextrous grippers exploiting nonholonomy of rolling. In particular, we have described a technique for dealing with objects of unknown shape, in order to reconstruct a mathematical model of their surface by performing rolling manipulation experiments, and an algorithm for planning rolling manipulation of objects with general surface. We have also described the implementation of devices designed to implement manipulation by rolling in practice, and described some experiments performed with these dextrous grippers. Several open problems remain to date. In particular, when connecting the exploratory technique described in section III to the planning algorithm described in IV, important questions arise as to the effects of reconstruction inaccuracies on planning. As it can be expected, it has been experimentally observed that such inaccuracies degrade the results of experimental execution of trajectories planned on the nominal reconstructed surface by some extent. Although in many cases this degradation would still be acceptable (this being the case in particular when planned manipulatory trajectories where rather simple), in general the problem of robustness of planning to modelling errors is a complex and widely open problem. A natural solution to such problem would be to implement feedback control strategies instead of open loop planning. However, at the state of the art, there is a lack of effective techniques for closed loop control and stabilization of rolling manipulation. Some steps in that direction have been undertaken by [37], who use the iterative replanning scheme of [38] for the stabilization of a sphere on a plane. Such scheme can in principle be extended to more general systems, provided suitable planners are available: the local-local property of the planning algorithm described in section IV is indeed potentially very useful in that regard. Future work will be devoted to inquire into these problems.

Acknowledgment

Raffaele Sorrentino and Marco Fedeli, former undergraduate students of the first author, are gratefully acknowledged for actively participating in the implementation of algorithms and devices described in this paper.

References

[1] A. Bicchi, "Hands for dextrous manipulation and powerful grasping: a difficult road towards simplicity," *tra*, vol. 16, no. 6, pp. 652–662, December 2000.

[2] A. Bicchi and K. Goldberg, Eds., *Proceedings of 1996 Workshop on Minimalism in Robotic Manipulation*. Proc. IEEE Int. Conf. on Robotics and Automation, 1996.

[3] M.T. Mason and J.K. Salisbury, *Robot hands and the mechanics of manipulation*, MIT Press, Cambridge (MA), 1985.

[4] D.J. Montana, "The kinematics of contact and grasp," *Int. Jour. of Robotics Research*, vol. 7, no. 3, pp. 17–32, 1998.

[5] C. Cai and B. Roth, "On the spatial motion of a rigid body with point contact," in *Proc. IEEE Int. Conf. on Robotics and Automation*, 1987, pp. 686–695.

[6] A. Cole, J. Hauser, and S.S. Sastry, "Kinematics and control of a multifingered robot hand with rolling contact," *IEEE Trans. on Robotics and Automation*, vol. 34, no. 4, pp. 398–404, 1989.

[7] Z. Li and J. Canny, "Motion of two rigid bodies with rolling constraint," *IEEE Trans. on Robotics and Automation*, vol. 6, no. 1, pp. 62–72, 1990.

[8] R. Sorrentino A. Bicchi, "Dexterous manipulation through rolling," in *Proc. IEEE Int. Conf. on Robotics and Automation*, 1995, pp. 452–457.

[9] A. Bicchi, D. Prattichizzo, and S.S. Sastry, "Planning motions of rolling surfaces," in *Proc. IEEE Int. Conf. on Decision and Control*, 1995.

[10] A.Marigo and A.Bicchi, "Rolling bodies with regular surface: Controllability theory and applications," *IEEE Trans. on Automatic Control*, vol. 45, no. 9, pp. 1586–1599, September 2000.

[11] M. Ceccarelli, A. Marigo, S. Piccinocchi, and A. Bicchi, "Planning motions of polyhedral parts by rolling," *Algorithmica*, vol. 26, no. 4, pp. 560–576, 2000.

[12] Y. Chitour, A. Marigo, and A. Bicchi, "Reachability and steering of rolling polyhedra: A case study in discrete nonholonomy," *IEEE Trans. on Automatic Control*, 2001, under revision.

[13] R.M. Murray, Z. Li, and S.S. Sastry, *A mathematical introduction to robotic manipulation*, CRC Press, Boca Raton, 1994.

[14] N. Sarkar, *Control of Mechanical Systems with Rolling Contacts: pplications to Robotics*, Ph.D. thesis, University of Pennsylvania, Computer and Information Science Department, 1993, Grasp Lab 357.

[15] O.D. Faugeras, M. Hebert, E. Pauchon, and J. Ponce, "Object representation, identification, and positioning from range data," in *Int. Symp. on Robotics Research*, M. Brady and R. Paul, Eds., pp. 425–446. MIT Press, 1984.

[16] R.C. Luo, W.H. Tsai, and J.C. Lin, "Object recognition with commbined tactile and visual information," in *Proc. Int. Conf. on Robot Vision and Sensory Control (ROVISEC)*, 1984, pp. 183–196.

[17] W.E.L. Grimson and T. Lozano-Pérez, "Model–based recognition and localization from sparse range or tactile data," *Int. J. of Robotics Research*, vol. 3, no. 3, pp. 3–35, 1984.

[18] R.E. Ellis, "Planning tactile recognition paths in two and three dimensions," *Int. J. of Robotics Research*, vol. 11, no. 2, pp. 87–111, 1992.

[19] M. Brady, J. Ponce, and A. Yuille, "Describing surfaces," in *Int. Symp. on Robotics Research*. 1984, MIT Press.

[20] W.E.L. Grimson, "On the recognition of parameterized objects," in *Int. Symp. on Robotics Research*. 1987, MIT Press.

[21] P.K. Allen, "Sensing and describing 3–d structure," in *Proc. IEEE Int. Conf. on Robotics and Automation*, 1986.

[22] P.K. Allen and K.S. Roberts, "Haptic object recognition using a multi–fingered dextrous hand," in *Proc. IEEE Int. Conf. on Robotics and Automation*, 1989.

[23] M.D. Berkemeyer and R.S. Fearing, "Determining the axis of a surface of revolution using tactile sensing," Tech. Rep. Memo no. UCB/ERL M89/117, EECS Dept. Univ. of California, Berkeley, 1989.

[24] S. Caselli, C. Magagnini, and F. Zanichelli, "On the robustness of haptic object recognition based on polyhedral shape representations," in *Proc. Int. Conf. on Intelligent Robots and Systems,*, IROS, 1995.

[25] A.N. Tikhonov and V.Y. Arsenin, *Solutions of Ill–Posed Problems*, W.H. Winston, Washington, D.C., 1977.

[26] G. Wahba, "Spline models for observational data," *SIAM, Series in Applied mathematics, Philadelphia*, vol. 59, 1990.

[27] T. Poggio and F. Girosi, "Networks for approximation and learning," *Proceedings of the IEEE*, vol. 78, no. 9, 1990.

[28] E. Sontag, "Control of systems without drift via generic loops," *IEEE Trans. on Automatic Control*, vol. 40, no. 7, pp. 1210–1219, 1995.
[29] H. Sussmann and Y. Chitour, "A continuation method for nonholonomic path–finding problems," in *Proc. IMA Workshop on Robotics*, 1993.
[30] A.W. Divelbiss and J. Wen, "Nonholonomic path planning with inequality constraints," in *Proc. IEEE Int. Conf. on Decision and Control*, 1993, pp. 2712–2717.
[31] S. Sekhavat and J. P. Laumond, "Topological properties for collision free nonholonomic motion planning: the case of sinusoidal inputs for chained form systems," *IEEE Transactions on Robotics and Automation*, vol. 14, no. 5, pp. 671–680, October 1998.
[32] A. Marigo, Y. Chitour, and A. Bicchi, "Manipulation of polyhedral parts by rolling," in *Proc. IEEE Int. Conf. on Robotics and Automation*, 1997, vol. 4, pp. 2992–2997.
[33] A. Schrijver, *Theory of Linear and Integer Programming*, Wiley Interscience Publ., 1986.
[34] M. Levi, "Geometric phases in the motion of rigid bodies," *Arch. Rational Mech. Anal.*, vol. 122, pp. 213–229, 1993.
[35] K. Nagata, "Manipulation by a parallel–jaw gripper having a turntable at each fingertip," in *Proc. IEEE Int. Conf. on Robotics and Automation*. IEEE, 1994, pp. 1663–1670.
[36] A. Bicchi, J. K. Salisbury, and D. L. Brock, "Contact sensing from force and torque measurements," *Int. Jour. of Robotics Research*, vol. 12, no. 3, pp. 249–262, June 1993.
[37] G. Oriolo and M. Vendittelli, "Robust stabilization of the plate-ball manipulation system," in *Proc. IEEE Int. Conf. on Robotics and Automation*, 2001, pp. 91–96.
[38] P. Lucibello and G. Oriolo, "Robust stabilization via iterative state steering with an application to chained-form systems," *Automatica*, vol. 37, pp. 71–79, 2001.

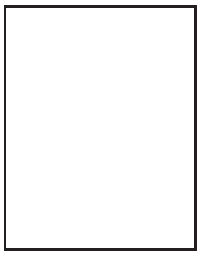

Alessia Marigo was born in Italy in 1969. She received the Laurea degree in Mathematics from the University of Pisa in 1994 and the Ph.D. degree in Robotics from the University of Genova in 1999. From 1995 to 1999 she worked on nonholonomic control systems and on discrete systems with quantized control at the Centro "E.Piaggio" of the University of Pisa. Since 1999 she is at SISSA/ISAS (International School for Advanced Studies) in Trieste, Italy. Her current research interests involve geometric control theory and applications.

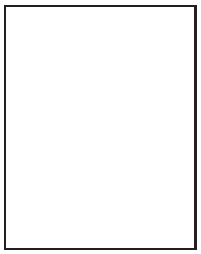

Antonio Bicchi received the Laurea degree (*cum laude*) from the University of Pisa in 1984, and the Ph.D. from the University of Bologna, in 1988. He has been a post–doctoral scholar at the Massachusetts Institute of Technology, Artificial Intelligence Laboratory, in 1988–1990.
He currently is an Associate Professor of System Theory and of Robotics, with the Department of Electrical Systems and Automation, University of Pisa, and the Interdept. Research Center "E. Piaggio", where he serves as Associate Director and leads the Robotics Group. He is a Senior Member of IEEE and an Associate Editor of the IEEE Trans. Robotics and Automation. His main research interests are in the field of dextrous manipulation, including force/torque and tactile sensing and sensory control; dynamics, kinematics and control of complex mechanichal systems; and motion planning and control for nonholonomic systems.